BIOCHEMISTRY
including biophysical chemistry & molecular biology

Article

pubs.acs.org/biochemistry

Dynamics of MutS–Mismatched DNA Complexes Are Predictive of Their Repair Phenotypes

Vanessa C. DeRocco,[†] Lauryn E. Sass,[†] Ruoyi Qiu,[§] Keith R. Weninger,*[,§] and Dorothy A. Erie*[,†,‡]

[†]Department of Chemistry and [‡]Curriculum in Applied Sciences and Engineering, The University of North Carolina at Chapel Hill, Chapel Hill, North Carolina 27599, United States

[§]Department of Physics, North Carolina State University, Raleigh, North Carolina 27695, United States

Supporting Information

ABSTRACT: MutS recognizes base–base mismatches and base insertions/deletions (IDLs) in newly replicated DNA. Specific interactions between MutS and these errors trigger a cascade of protein–protein interactions that ultimately lead to their repair. The inability to explain why different DNA errors are repaired with widely varying efficiencies *in vivo* remains an outstanding example of our limited knowledge of this process. Here, we present single-molecule Förster resonance energy transfer measurements of the DNA bending dynamics induced by *Thermus aquaticus* MutS and the E41A mutant of MutS, which is known to have error specific deficiencies in signaling repair. We compared three DNA mismatches/IDLs (T-bulge, GT, and CC) with repair efficiencies ranging from high to low. We identify three dominant DNA bending states [slightly bent/unbent (**U**), intermediately bent (**I**), and significantly bent (**B**)] and find that the kinetics of interconverting among states varies widely for different complexes. The increased stability of MutS–mismatch/IDL complexes is associated with stabilization of **U** and lowering of the **B** to **U** transition barrier. Destabilization of **U** is always accompanied by a destabilization of **B**, supporting the suggestion that **B** is a "required" precursor to **U**. Comparison of MutS and MutS-E41A dynamics on GT and the T-bulge suggests that hydrogen bonding to MutS facilitates the changes in base–base hydrogen bonding that are required to achieve the **U** state, which has been implicated in repair signaling. Taken together with repair propensities, our data suggest that the bending kinetics of MutS–mismatched DNA complexes may control the entry into functional pathways for downstream signaling of repair.

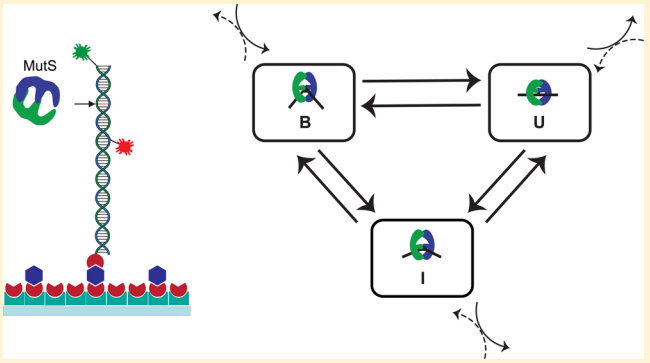

Maintaining the integrity of the DNA genome is essential to all organisms. Not only is DNA continuously subjected to assaults from endogenous and exogenous chemicals, but the fidelities of DNA polymerases are not sufficiently high to generate error-free copies of the DNA during replication. Multiple DNA repair pathways have evolved to counter these challenges. DNA mismatch repair (MMR) proteins identify and correct DNA synthesis errors that occur during replication. These proteins also participate in DNA damage-induced activation of cell-cycle checkpoints and apoptosis, as well as several other DNA transactions. Inactivation of MMR genes not only dramatically increases the frequency of mutations but also decreases the level of apoptosis, increases the level of cell survival, and results in resistance to many chemotherapeutic agents.[1−3] In humans, mutations in genes responsible for the initiation of MMR are associated with >80% of hereditary nonpolyposis colorectal cancers (HNPCCs) and certain sporadic cancers.[4−6]

MMR is initiated by MutS and MutL homologues, which are highly conserved throughout prokaryotes and eukaryotes. They are both dimers and contain DNA binding and ATPase activities that are essential for MMR *in vivo*.[7] The MMR cascade is initiated after MutS binds specifically to a mismatch or base insertions/deletions (IDLs). Productive mismatch recognition leads to an ATP-dependent conformational change in MutS, inducing formation of a mobile clamp state that can move along the DNA. This activated state of MutS, in turn, interacts with MutL, promoting the downstream events that lead to repair.[7,8]

Crystal structures of *Thermus aquaticus* and *Escherichia coli* MutS and human MutSα bound to a number of different mismatched DNA bases and IDLs[9−12] reveal that only two specific amino acid contacts are made between MutS or MutSα and the mismatched base. These contacts are located in a conserved Phe-Xaa-Glu motif, where the phenylalanine stacks with the mismatched base and the glutamate forms a hydrogen bond with N3 of the mismatched pyrimidine or N7 of the mismatched purine[9−12] (Figure 1A). All other interactions between MutS and the DNA are nonspecific backbone contacts. These specific and nonspecific interactions induce a

Received: October 21, 2013
Revised: January 24, 2014
Published: March 4, 2014

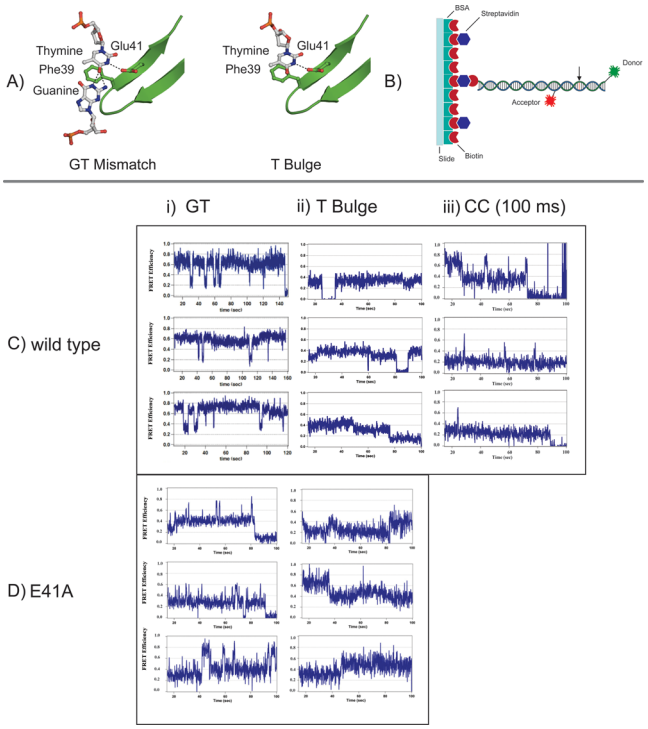

Figure 1. Representative single-molecule FRET traces for MutS and MutS-E41A bound to GT, T-bulge, and CC mismatch DNA. (A) Models illustrating the interactions between Phe39 and Glu41 of *Taq* MutS and a GT mismatch or a T-bulge. The *Taq* MutS−T-bulge structure is derived from Protein Data Bank entry 1EWQ.[11] The *Taq* MutS−GT structure is a model derived from aligning the recognition motifs of *E. coli* MutS GT (Protein Data Bank entry 1E3M)[10] with the *Taq* MutS−T-bulge structure (Protein Data Bank entry 1EWQ).[11] Molecular models were created using PyMOL Molecular Graphics System, version 1.3 (Schrödinger, LLC). (B) Cartoon illustrating the 50 bp DNA substrate used in single-molecule FRET studies. DNA was immobilized via a biotin and streptavidin surface functionalization. A TAMRA or Cy3 donor dye is located at the 3′ end, and a Cy5 acceptor dye is located 19 bases from the donor. (C and D) Example smFRET traces for MutS and MutS-E41A, respectively, in the presence of (i) GT, (ii) T-bulge, and (iii) CC. Acceptor or donor blinking causes excursions to zero FRET in some traces. Each tick mark on the x-axis represents 20 seconds.

sharp bend (or kink) in the DNA at the mismatch site. Atomic force microscopy (AFM), single-molecule Förster resonance energy transfer (smFRET), and small-angle X-ray scattering (SAXS) studies have revealed that MutS−mismatch complexes adopt multiple bent conformations as well as an unbent (or slightly bent) conformation, which exist in dynamic equilibrium.[13−16] Notably, for prokaryotic MutS, mismatch recognition does not necessarily lead to sliding clamp formation and repair,[17−21] and the unbent conformation has been proposed to be a necessary precursor to the formation of the ATP-induced sliding clamp state that signals repair.[13,14,18] Overall, DNA bending and unbending at mismatches have been proposed to play a fundamental role in mismatch recognition or subsequent repair signaling.[7,22]

Here, we report smFRET measurements of the conformational dynamics for *T. aquaticus* MutS (MutS) and a MutS mutant, in which the Glu in the Phe-Xaa-Glu mismatch recognition motif is changed to Ala (MutS-E41A), bound to different DNA mismatches. We examine the DNA bending dynamics of MutS bound to a single T insertion (T-bulge), a GT mismatch, and a CC mismatch and those of MutS-E41A bound to a T-bulge and a GT mismatch. We chose these complexes because studies of MutS and its homologues indicate that MutS−T-bulge, MutS−GT, and MutS-E41A−T-bulge complexes are competent to signal repair, whereas MutS−CC and MutS-E41A−GT complexes are impaired with respect to signaling repair.[17−21] As outlined in Table 1, comparison of the properties of these complexes allows us to begin to dissect the roles of base−base and MutS-E41−base hydrogen bonding in determining the MutS−mismatch conformations, and how these conformations correlate with repair signaling. To examine the recognition states that precede the formation of the ATP-induced sliding clamp, we examine the conformational dynamics of MutS−mismatch complexes in the absence of nucleotide cofactors.

By monitoring changes in DNA bending upon MutS binding as well as the subsequent equilibrium DNA bending dynamics, we characterized the conformational states and pathways associated with recognition of the different mismatches by MutS and MutS-E41A. The conformational dynamics of all the complexes can be described in terms of three classes of DNA conformations: slightly bent/unbent (**U**), intermediately bent (**I**), and strongly bent (**B**); however, the relative stabilities of these states and their rates of interconversion vary dramatically for the different complexes. Comparison of the conformational properties of the wild-type and mutant MutS−mismatch complexes with their abilities to signal repair supports the idea that the slightly bent/unbent state (**U**) must be sufficiently populated to signal repair[13,18] and provides a mechanistic model of how **U** is achieved. Taken together, our data suggest that the dynamics of MutS−mismatch/IDL complexes may be a key factor in the overall ability of the MMR system to repair certain types of mismatches.

Table 1. Summary of Implications of Comparisons of Experiments

	hydrogen bonding	repair signaling	conformational properties
comparing T-bulge to GT	probes role of base−base hydrogen bonding (base stacking may also play a role)	both are well repaired	longer-lived, less bent states for T-bulge than for GT
comparing T-bulge and GT to CC	not applicable	T-bulge and GT efficiently repaired; CC poorly repaired	very short binding times and only bent states on CC compared to bent and unbent states on the T-bulge and GT
comparing flow to steady state for GT and T-bulge	not applicable	not applicable	observed initial conformational state upon binding differs between GT and T-bulge
comparing wild-type MutS to MutS-E41A	probes hydrogen bonding between Glu41 and the mismatched base	E41A signals repair on the T-bulge; E41A impaired for repair signaling on GT	loss of the Glu hydrogen bond to the mismatched base has minimal effect on T-bulge conformations but alters GT conformations and increases the conformational dynamics of both T-bulge and GT complexes

dx.doi.org/10.1021/bi401429b | *Biochemistry* 2014, 53, 2043−2052

EXPERIMENTAL PROCEDURES

Protein and DNA Substrates. Wild-type MutS and MutS-E41A from *T. aquaticus* were overexpressed in *E. coli* and purified as previously described.[23] High-performance liquid chromatography-purified single-stranded oligonucleotides (labeled and unlabeled as indicated) were purchased from Integrated DNA Technologies and TriLink Biotechnologies. Oligonucleotide names and sequences are listed in Table 2. The location of the DNA mismatch is noted at the underlined base. DNA substrates containing a TAMRA-labeled oligonucleotide (Table 2, A1) or a Cy3-labeled oligonucleotide (Table 2, A2) were annealed to a Cy5-labeled oligonucleotide (Table 2, C1-GT, C2-T-bulge, and C3-CC) to create a duplex DNA fragment containing the desired mismatch (Figure 1B). Oligonucleotides were annealed in buffer containing 20 mM Tris-HCl (pH 7.8), 100 mM sodium acetate, and 5 mM magnesium chloride in a 1:1 ratio at 65 °C for 20 min followed by slow cooling. When the temperature reached 55 °C, an additional unlabeled complementary oligonucleotide (Table 2, B1) was added and annealed to complete the duplex DNA substrate. The substrate was allowed to slowly cool to room temperature and was stored on ice or at 4 °C.

Table 2. Sequences of DNA Oligonucleotides Used in smFRET Experiments[a]

oligo	sequence (5′ to 3′)
A1	biotin-TGT CGG GGC TGG CTT AAG GTG TGA AAT ACC TCA TCT CGA GCG TGC CGA TA-TAMRA
A2	biotin-TGT CGG GGC TGG CTT AAG GTG TGA AAT ACC TCA TCT CGA GCG TGC CGA TA-Cy3
B1	AGG TAT TTC ACA CCT TAA GCC AGC CCC GAC A
C1-GT	TAT CGG CAC GTT CGA GAT G-Cy5
C2-T-bulge	TAT CGG CAC GTC TCG AGA TG-Cy5
C3-CC	TAT CGG CAC CCT CGA GAT G-Cy5

[a]All sequences are shown in the 5′ to 3′ order with biotin and fluorophore labels noted at the appropriate positions. The locations of mismatch sites are noted as underlined bases.

Fluorescence Microscopy. Quartz microscope slides and flow channels were prepared as previously described.[14,24] For DNA immobilization, the quartz surface was treated first with biotinylated BSA (Sigma, 1 mg/mL, 5 min incubation) followed by streptavidin (Invitrogen, 0.1 mg/mL, 5 min incubation), similar to methods previously described.[14] Annealed biotinylated, fluorescently labeled, mismatched DNA was added to the treated surfaces at a concentration ranging from 10 to 30 pM for 5 min, and the unbound DNA was removed by rinsing with chilled buffer [20 mM Tris-HCl (pH 7.8), 100 mM NaOAc, and 5 mM $MgCl_2$]. Samples were imaged at room temperature in the rinsing buffer described above upon addition of enzymatic oxygen-scavenging components [2% glucose (Sigma), 1% β-mercaptoethanol (Fluka), 0.1 mg/mL glucose oxidase (Sigma), and 0.025 mg/mL catalase (Sigma)] to enhance the fluorophore lifetime and upon addition of triplet-state quencher cyclooctatetraene (Sigma-Aldrich) (~50 μM). Images were collected in the presence and absence of 200 nM MutS. MutS was allowed to bind the DNA for at least 5 min prior to the collection of images for steady-state experiments. Protein was added through a flow-cell apparatus for flow binding experiments while imaging in real time.

Data were collected using a prism-type total internal reflection fluorescence (TIRF) laser microscope operating with alternating 532 and 635 nm illumination, as described previously.[24] Fluorescence emission was collected with a 60× 1.2 NA water immersion objective and split by a 645dcrx dichroic mirror (Chroma) into short and long wavelength paths, filtered for TAMRA and Cy5 emissions using HQ 585/70 and HQ 700/75 bandpass filters (Chroma), and relayed as side-by-side images onto a charge-coupled device camera (Cascade 512B, Roper Scientific). Images were collected at 10 or 66 frames per second (100 or 15 ms frame rate, respectively) using software written in house.

Observed intensities of single molecules were integrated with software written in house to obtain individual fluorescence emission time traces as described previously.[24] Emission traces were background subtracted and corrected for leakage of the donor signal into the acceptor channel (~5%). Molecules not confirmed to contain exactly one donor and one acceptor fluorophore were excluded from further analysis. FRET efficiencies were calculated from the respective donor and acceptor emissions as $E = I_A/(I_D + I_A)$, where I_D and I_A are the corrected intensities of the donor fluorophore and acceptor fluorophore, respectively.

FRET Data Analysis. We apply a Gaussian derivative kernel algorithm to isolate FRET transitions in single-molecule traces.[25] This algorithm (as previously described and available at http://www.cs.unc.edu/~nanowork/cismm/download/edgedetector/index.html) yields each FRET efficiency sampled in a given FRET trace as well the time the molecule spends at that FRET efficiency ("dwell time", or Δt) and the transition sequence.[14] Data for the MutS-E41A–GT complex underwent an additional analysis for short-lived transitions using hidden Markov modeling (HaMMy version 4.0 acquired from http://bio.physics.illinois.edu/HaMMy.html).[26] FRET transitions are used to generate transition density plots (TDPs), and lifetimes are used to assess the kinetics of the different conformations sampled for a given MutS–DNA complex. Details of this analysis approach have been previously described.[14] Histogram distributions are generated from the average FRET value of each transition in a given single-molecule FRET trace identified using the Gaussian derivative algorithm. FRET values in histograms and TDPs are not weighted with respect to the lifetime of a state.

RESULTS

We used smFRET to characterize the DNA conformations sampled when MutS or MutS-E41A is bound to three different DNA mismatches/IDLs that exhibit differences in repair properties: a single-thymine insertion (T-bulge), a GT mismatch, and a CC mismatch.[17,18,20,21,27] We employed 50 bp double-stranded DNA substrates, labeled with a FRET acceptor dye (Cy5) on one end, a FRET donor dye (TAMRA) 19 bases 3′ of the acceptor dye, and a mismatch located midway between the dyes.[14] In addition, the 5′ end of the DNA is biotinylated to allow immobilization on a quartz substrate (Figure 1B and Experimental Procedures). Changes in smFRET signals represent changes in DNA bending (and/or twisting).[14]

MutS–DNA Conformations and Conformational Dynamics Exhibit Mismatch Specific Behavior. Figure 1 shows representative FRET traces for T-bulge, GT, and CC DNA mismatches in the presence of MutS (Figure 1C) or MutS-E41A (Figure 1D). Inspection of the individual time

dx.doi.org/10.1021/bi401429b | Biochemistry 2014, 53, 2043–2052

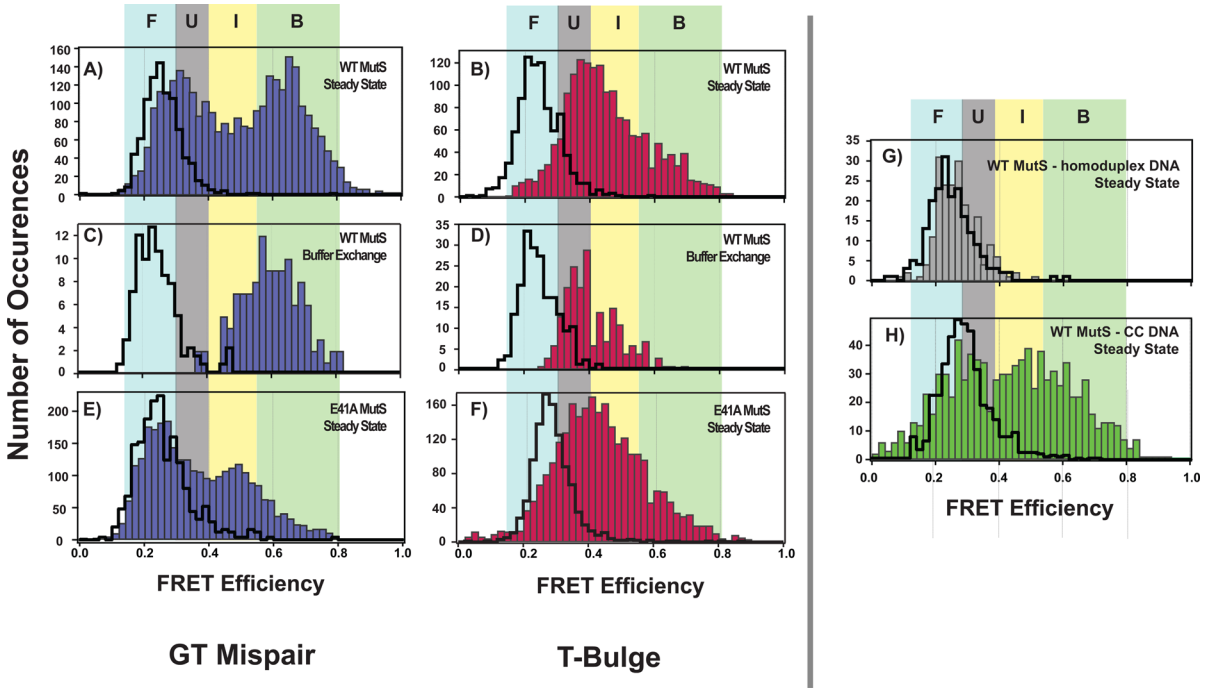

Figure 2. Distributions of smFRET efficiencies for MutS− and MutS-E41A−mismatch complexes. Histograms of steady-state distributions of observed FRET efficiencies for MutS bound to GT (A) (n = 2992), T-bulge (B) (n = 1664), homoduplex DNA (G) (n = 200), and CC (H) (n = 909) and for MutS-E41A bound to GT (E) (n = 2931) and T-bulge (F) (n = 2680), respectively. Histograms of the distributions of FRET efficiencies induced upon MutS binding to GT (C) and T-bulge (D) during buffer exchange experiments are displayed. For each histogram, black cityscapes indicate the distribution of the observed innate FRET for the TAMRA-Cy5-labeled DNA substrate in the absence of protein and colored bars represent the distribution of FRET in the presence of the indicated protein. Histogram values are determined as described in Experimental Procedures and are not scaled by the dwell times of MutS on the DNA. The proposed MutS−DNA bending states are outlined for each distribution: **F**, free DNA; **U**, unbent state; **I**, intermediately bent state; **B**, bent state. The data for the steady-state experiments with MutS−GT complexes were taken from ref 14.

traces reveals that MutS−DNA complexes sample different conformations and exhibit different rates of switching between FRET states for the three mismatches.

As previously described,[14] MutS−GT complexes (Figure 1Ci) sample six different conformational states, with rates of interconversion between states ranging from 0.002 to 0.6 s^{-1}. The stability and the rates of transitions between states of the MutS−GT complex are optimally matched to the detection capability of our single-molecule fluorescence assay (given the limitations of fluorophore photobleaching and emCCD-based detection), which allowed the complete conformational landscape to be characterized in detail.[14] In contrast, MutS−T-bulge complexes are significantly more stable and exhibit fewer conformational transitions with smaller changes in DNA bending, limiting our ability to identify poorly populated, closely spaced states and to evaluate the complete kinetic landscape of these complexes. Most MutS−T-bulge FRET traces (Figure 1Cii) displayed a constant FRET state over the observation period, which is limited by dye photobleaching. Approximately 20% of the complexes showed one or two FRET transitions during the observation time (approximately 100 s). The CC mismatch represents the other end of the kinetic spectrum, where MutS appears to be bound only for a short period, usually a few frames at an acquisition rate of 10 Hz (Figure 1Ciii). Consequently, we used faster camera frame rates (Figure 1 of the Supporting Information) and determined the lifetime to be ∼80 ms for MutS bound to CC. This short binding time is consistent with the weak binding affinity of *T. aquaticus* MutS for a CC mismatch (K_d = 720 nM).[28]

Figure 2 shows histograms of the populations of FRET states sampled for MutS−homoduplex, MutS−GT, MutS−T-bulge, and MutS−CC complexes. The MutS−homoduplex DNA complexes do not exhibit a significant shift away from the FRET of free DNA (Figure 2G), as seen previously.[14] Also consistent our previous observations,[14] no variation in fluorescence intensity was observed with homoduplex DNA in the presence or absence of MutS, confirming little direct binding of MutS to the fluorophores altering quantum yields in this study (Figure 2 of the Supporting Information). In contrast, the FRET distributions vary widely among the MutS−GT, MutS−T-bulge, and MutS−CC complexes (Figure 2A,B,H). The distribution of MutS−GT FRET values is very broad, covering six different states.[14] Like that of the MutS−GT complex, the distribution of the MutS−T-bulge complex (Figure 2B) is also broad, consistent with multiple bent states; however, the distribution is shifted to lower FRET values relative to those of the MutS−GT complex. This result is consistent with AFM analysis of DNA bend angles, which showed that MutS−T-bulge complexes were less bent than MutS−GT complexes.[13,18]

Our smFRET measurements of CC DNA in the absence of MutS (Figure 2H) are shifted to slightly higher FRET values with a modestly larger width compared to those of GT or T-bulge substrates, consistent with free DNA having increased flexibility at the CC mismatch.[29] MutS−CC complexes (Figure 2H) show two peaks: one overlapping free DNA and a broad peak ranging from FRET values of 0.4 to 0.8. The fraction of events overlapping free DNA for each mismatch is consistent

dx.doi.org/10.1021/bi401429b | *Biochemistry* 2014, 53, 2043−2052

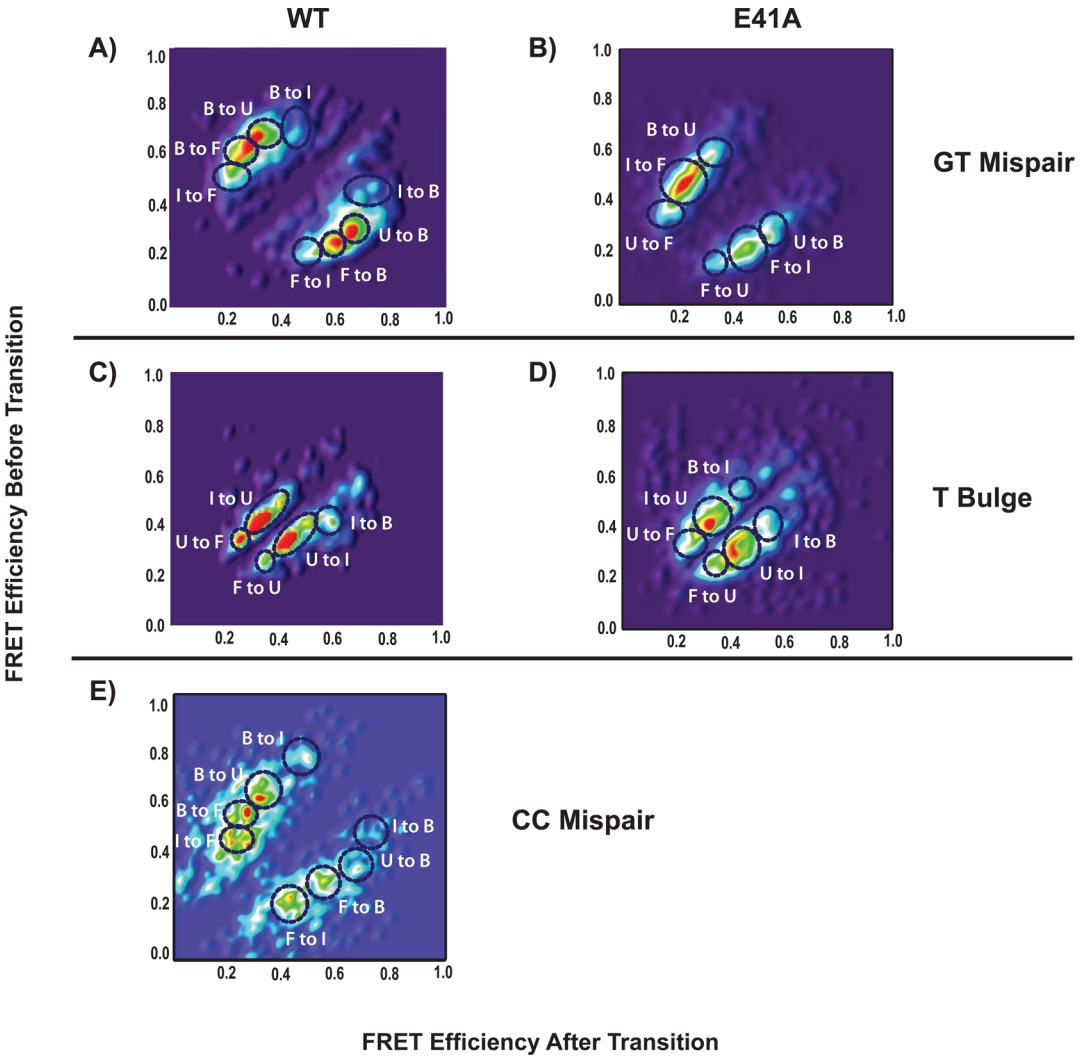

Figure 3. Transition density plots for MutS and MutS-E41A in the presence of GT, T-bulge, and CC mismatch DNA. TDPs of FRET changes observed due to conformational changes and protein binding and unbinding for MutS in the presence of GT (A) (n = 2535 transitions), a T-bulge (C) (n = 2046 transitions), or a CC (E) (n = 899 transitions) and for MutS-E41A in the presence of a GT (B) (n = 2046 transitions) or a T-bulge (D) (n = 1672 transitions). TDPs were generated from FRET transitions identified using a Gaussian derivative kernel algorithm described previously.[14] The specific transitions between states are circled: **F**, free DNA; **U**, slightly bent/unbent state; **I**, intermediately bent state; **B**, bent state. The data for MutS−GT complexes were taken from ref 14.

with their relative binding affinities (K_d values of 5 nM for the T-bulge, 40 nM for GT, and 720 nM for CC)[14,28,30−32] and our experimental MutS concentration (200 nM). CC has the most events overlapping with free DNA, and the T-bulge has the fewest.

Analysis of plots of the FRET values before and after transitions between states [so-called transition density plots (TDPs)] (Figure 3) reveals the prevalence of the conformational transitions for MutS bound to different mismatches. In addition, the TDPs are particularly useful for identifying states with closely spaced FRET values, which can overlap in the histograms.[26] For example, the MutS−T-bulge complexes show only small changes in FRET, preferentially sampling two FRET states centered at FRET values of ∼0.36 and ∼0.46 (Figure 3C). These states overlap in the broad peak in the histogram but can clearly be observed in individual traces (Figure 1Cii) and the TDPs (Figure 3). Six conformational states have been identified for MutS−GT complexes.[14] Independent analysis of the MutS−T-bulge complexes identified three distinct conformational states with variable degrees of bending (**B**, **I**, and **U**). Despite the short binding time for binding of MutS to the CC mismatch, we also identified two bending states (**B** and **I**) that overlap with the states independently found for the T-bulge and the GT mismatch complexes.

Although we have identified six states for MutS−GT complexes, some of these states had overlapping FRET values that could be separated only by careful kinetic analyses.[14] The slow MutS−T-bulge and fast MutS−CC kinetics prevented the separation of those overlapping FRET states. The FRET values of the poorly populated MutS−GT states are contained within the three states (**B**, **I**, and **U**) identified for the T-bulge− and CC−MutS complexes. In fact, the conformational properties of both wild-type and mutant (see below) MutS bound to all of the mismatches studied can be effectively compared using these three dominant classes of DNA conformations: unbent/slightly bent (**U**; FRET values of 0.30−0.40), intermediately bent (**I**; FRET values of 0.4−0.55), and significantly bent (**B**; FRET values of >0.55) (Figures 2 and 3). Quantitative analysis of the transitions among these states and free DNA (F) (see below)

dx.doi.org/10.1021/bi401429b | *Biochemistry* 2014, 53, 2043−2052

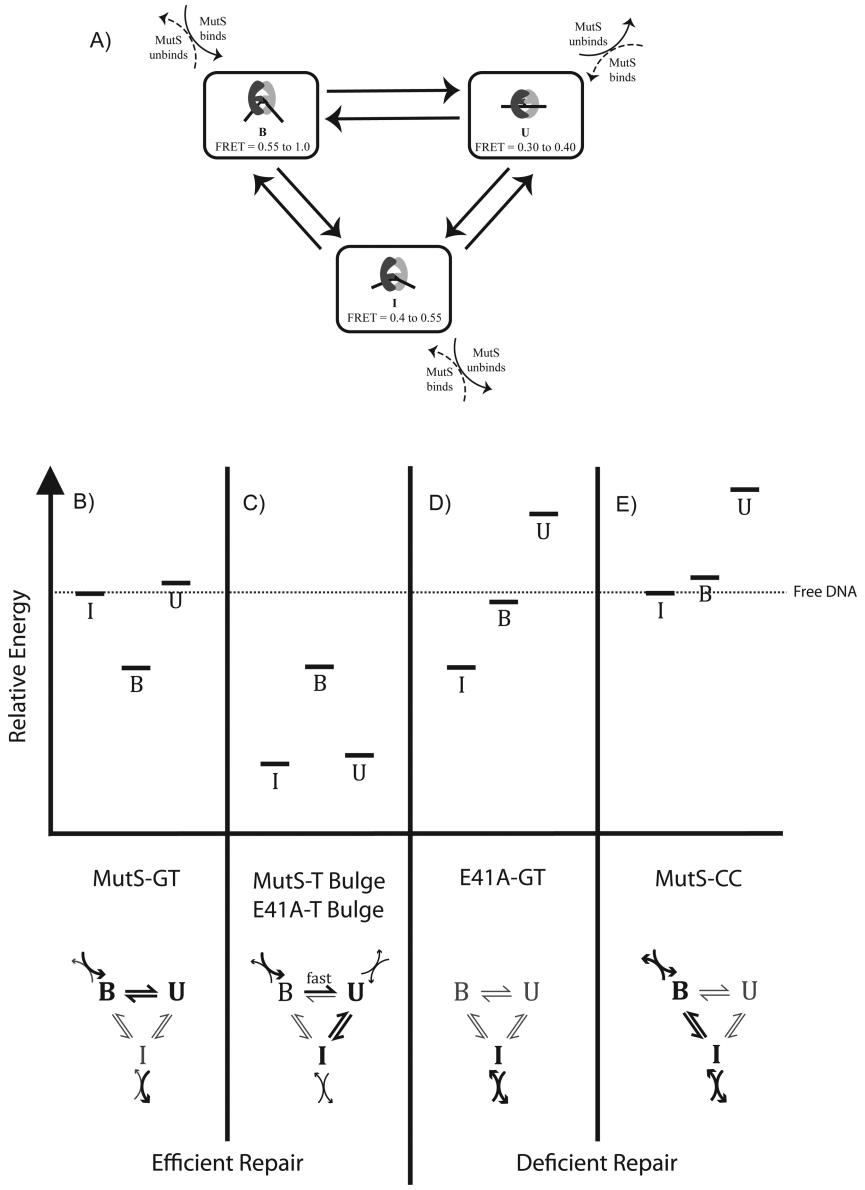

Figure 4. Relative stabilities of states for MutS− and MutS-E41A−DNA complexes. (A) Mechanistic depiction of MutS−DNA conformational states, including energy level diagrams representative of the relative stabilities of **U**, **I**, and **B** states for (B) the MutS−GT complex, (C) the MutS−T-bulge and MutS-E41A−T-bulge complexes, (D) the MutS-E41A−GT complex, and (E) the MutS−CC complex. The relative stabilities of the states are estimated on the basis of the changes in their occupancies relative to those of the MutS−GT complexes for which we were able to obtain quantitative kinetic data.[14] The data for MutS−GT complexes were taken from ref 14.

allows estimation of their relative stabilities and determination of their conformational pathways (Figure 4).

MutS−GT and MutS−T-bulge complexes exhibit multiple conformational states; however, each complex switches back and forth between two dominant states. MutS−GT complexes show relatively rapid transitions between **B** and **U** (with large changes in DNA bending), with rare transitions to **I**. In contrast, the more stable MutS−T-bulge complexes (K_d values of 5 nM for the T-bulge and 40 nM for GT)[30] rarely populate **B** and undergo infrequent transitions between the long-lived conformational states, **I** and **U** (with only small changes in DNA bending). Interestingly, the long dwell times and infrequent transitions between states **I** and **U** for the T-bulge are similar to the transition rates between states **I** and **U** determined for GT (0.05 s^{-1} for **U** to **I** and 0.02 s^{-1} for **I** to **U**).[14] Notably, for MutS−GT complexes, **I** is not on path to formation of **U** because MutS preferentially dissociates from **I** (Figure 4); however, the increased stability of the MutS−T-bulge complex relative to those of MutS−GT complexes results in **I** preferentially undergoing the transition to **U** instead of dissociating, and **I** becomes on path to **U** for MutS−T-bulge complexes. These results suggest that the 8-fold increase in binding affinity of MutS for a T-bulge relative to a GT results from the stabilization of states **I** and **U** but not **B** (Figure 4A,B).

The transitions for CC are dominated by short binding events (Figure 3E). MutS binds to **I** and **B** with similar frequencies and dwell times, suggesting that **I** and **B** have similar stabilities, and **U** is rarely observed (Figures 2 and 3). The smFRET histograms for experiments with the CC mismatch acquired at 15 ms using a different donor−acceptor pair with a different FRET scaling (Figure 1 of the Supporting Information) display a distinct gap between FRET DNA values

dx.doi.org/10.1021/bi401429b | *Biochemistry* 2014, 53, 2043−2052

and higher FRET values that clearly illustrates the low probability of visiting **U** as compared to the other mismatches where the higher FRET values in the histograms smoothly overlap with those of the free DNA state. These results can be explained if the 18-fold lower binding affinity of MutS for CC relative to that for GT (K_d values of 40 nM for GT and 720 nM for CC)[14,28,30−32] results from destabilization of both **B** and **U** but not **I** (Figure 4).

Flow Experiments Reveal Different Initial Conformations for Binding of MutS to GT and the T-Bulge. All of the conformational dynamics discussed above were determined from steady-state studies, where MutS was preincubated with the DNA prior to single-molecule imaging and was present in solution during imaging. This steady-state protocol limits our level of confidence in assigning binding events for GT mismatches, and because of the high affinity of MutS for T-bulge mismatches, binding events are rarely observed for the T-bulge in steady-state experiments. Consequently, to unequivocally identify the initial binding conformations induced by MutS, we directly monitored the first DNA conformation induced at the mismatch upon MutS binding, by imaging immobilized DNA in a flow chamber while adding MutS in real time (Figure 2C,D).

The distribution of FRET states adopted upon binding of MutS to the GT mismatch (Figure 2C) indicates that it preferentially binds to the bent states (**B** and **I**) observed in the steady-state experiments (Figure 2A). This observation is consistent with our previous conclusion, based on steady-state data, that MutS preferentially binds GT in **B** and then undergoes the transition to **U**.[14] In contrast, the distribution of FRET states for binding of MutS to a T-bulge (Figure 2D) shows that MutS binds preferentially to the less bent state (**U**) of the two dominant populations (**U** and **I**) in the steady-state experiments.

MutS-E41A−DNA Complexes Exhibit Wild-Type-like Conformations on a T-Bulge but Not on a GT Mismatch. The distribution of FRET states visited for MutS-E41A−T-bulge complexes (Figure 2F) is similar to the distribution for MutS−T-bulge complexes (Figure 2B). As shown in FRET traces of individual molecules (Figure 1D), MutS-E41A−T-bulge complexes are more dynamic than MutS−T-bulge complexes, with the dominant transition between **U** and **I** occurring with a greater frequency (20% of the MutS−T-bulge complexes and 50% of the MutS-E41A−T-bulge complexes showed transitions during our observation window of 100 s). Despite this difference in dynamics, the overall distributions of transitions among FRET states for MutS and MutS-E41A bound to the T-bulge are very similar (Figure 3C,D). These results indicate that the same states and transitions occur for both the MutS− and MutS-E41A−T-bulge complexes, only with faster dynamics for the MutS-E41A complex. Taken together with the similar binding affinities of MutS and MutS-E41A for a T-bulge,[18] these results suggest that mutation of Glu to Ala does not significantly alter the stabilities of **U**, **I**, and **B** but slightly lowers the transition barriers between **U** and **I** (Figure 4).

In contrast to the similarity of conformational states for MutS− and MutS-E41A−T-bulge complexes, MutS− and MutS-E41A−GT complexes exhibit both different distributions and different lifetimes of states (Figures 1−3). Two of the most stable states (**B** and **U**) and the dominant transition (**B** to **U**) that are seen for the MutS−GT complex are rarely observed for the MutS-E41A−GT complex, where the dominant transitions are binding to **I** and unbinding from **I** (Figures 2 and 3). Although **B** is populated for MutS-E41A−GT complexes, its lifetime is dramatically shortened compared to that of MutS−GT complexes, in which it is the longest-lived state (Figure 1Di). In fact, **B** is so short-lived for MutS-E41A−GT complexes that it is not efficiently detected by our edge detection algorithm, which uses a five-point window. Consequently, **B** is underrepresented in the population histogram (Figure 2E), although transitions to and from it are visible upon inspection of individual traces (Figure 1Di). To improve the detection of these fast transitions, we used hidden Markov modeling-type analysis (Experimental Procedures)[26] of these fast transitions to verify that the most common transition from **B** is unbinding. In MutS-E41A−GT complexes, **U** can be visited via a transition from **B**, but with a greatly reduced frequency relative to that of MutS−GT complexes (Figure 3). The observed reduction in the level of complexes in **U** and the increase in the level of complexes in **I** are consistent with previous AFM studies, which showed a shift of the unbent population to ∼15°.[18] These results, taken together with the similar binding affinities of MutS and MutS-E41A for GT, suggest that **B** and **U** are destabilized and **I** is stabilized for MutS-E41A−GT complexes relative to MutS−GT complexes (Figure 4).

DISCUSSION

Previous smFRET, AFM, and SAXS studies of *Taq* and *E. coli* MutS indicate that MutS−mismatch complexes adopt multiple conformations, with different extents of DNA bending,[13−16,18] and that the time scales of interconversion of these states can vary by 2 orders of magnitude.[14] In addition, it has been suggested that MutS bends homoduplex DNA while searching for a mismatch and, upon recognition of a mismatch, undergoes a two-step transition via a kinked intermediate to a slightly bent/unbent conformation.[13,18] Formation of this unbent conformation is proposed to be essential for the ATP activation of MutS that signals repair.[13,18] Our current data, which significantly expand on these previous studies, both support the idea that sufficient sampling of an unbent (or slightly bent) conformation is necessary for signaling repair and provide insight into the mechanisms by which signaling may be impaired. In particular, we find that the dynamics of the MutS−mismatched DNA complexes are predictive of the differential abilities of wild-type and mutant MutS−mismatch/IDL complexes to undergo the ATP-induced formation of the sliding clamp that signals repair.

Although MutS efficiently undergoes the conformational change to the sliding clamp state that signals repair on both the T-bulge and GT, the mutant MutS-E41A can undergo this conformational change on a T-bulge but not on a GT, even though MutS-E41A exhibits binding affinities for both substrates similar to those of MutS.[18,21] Interestingly, we find that removal of E41, which makes a hydrogen bond to the mismatch or IDL base, increases the conformational dynamics of both T-bulge and GT complexes (Figure 1D). For the T-bulge, transitions between states occur approximately twice as often for MutS-E41A as for MutS, but this increase in dynamics does not significantly alter the occupancies of the different conformational states (Figure 2) or the dominant transitions, which are between **I** and **U** (Figure 3). These results indicate that E41 plays only a small role in dictating MutS−T-bulge conformational properties and are consistent with the wild-type-like signaling behavior of MutS-E41A on a T-bulge.[18,20] In contrast, MutS-E41A−GT complexes show both different

distributions of conformations and different conformational dynamics relative to those of MutS−GT complexes. For MutS−GT complexes, **B** is the most stable state and the dominant transition is **B** to **U**, whereas for MutS-E41A−GT complexes, **B** is only briefly visited and ***U*** is rarely observed. In addition, the dominant transitions are binding to **I** and unbinding from **I** (Figures 2 and 3), which is the most stable state for MutS-E41A−GT complexes (Figure 4).

The different properties of MutS-E41A on a GT and T-bulge suggest that formation of both **B** and **U** involves changes in base−base hydrogen bonding (although base stacking also could be playing a role). Specifically, removal of the interaction between the T-bulge and E41 minimally affects the conformational properties of MutS bound to a T-bulge, which does not have a hydrogen-bonding partner, whereas removal of this interaction greatly affects the properties of MutS bound to a GT, which makes two base−base H-bonds. If **B** represents the conformation observed in the crystal structures of MutS−mismatch complexes, it is not surprising that removal of E41 reduces its stability, because the bent conformation seen in the crystal structures reveals significant changes in base−base hydrogen bonding relative to that of free DNA. Interestingly, loss of this hydrogen bonding interaction appears to stabilize **I** for the MutS−GT complexes (Figure 4), indicating that E41 inhibits the formation **I** for the GT complexes.

A similar analysis can be applied to the binding of MutS to a CC mismatch, which is also thought to be impaired for signaling.[17,19] In the case of MutS−CC complexes, however, the stability of the complex is greatly reduced (K_d = 720 nM), with the stability of both **B** and **U** lowered relative that of the MutS−GT complex. As a result, MutS exhibits very short dwell times (<1 s), binding to both **B** and **I** but not **U**. Taken together with our MutS-E41A results, the concomitant destabilization of **U** and **B** for both MutS−CC and MutS-E41A−GT complexes support the idea that **B** is a required precursor to the formation of **U** and that **I** is off path, except for the case in which the complexes are extremely stable (e.g., MutS−T-bulge complex).

Our flow experiments following binding of MutS to GT show that MutS preferably binds in **B** and then undergoes the transition to **U**, supporting the suggestion that **B** is an intermediate in the formation of **U**. In contrast, MutS appears to preferentially bind a T-bulge in **U** and remains stably bound with occasional transitions to **I**, which is also long-lived, and **B** is rarely populated (Figures, 2B,D and 3C). The observation that MutS binds to a T-bulge directly into **U** suggests either that MutS recognition of a T-bulge follows a pathway different from that of MutS recognition of a GT or that MutS follows the same conformational pathway for recognition of both GT and the T-bulge but the transition from **B** to **U** is too fast to observe for the T-bulge in these experiments. This latter idea is supported by previous studies that strongly suggest that MutS searches DNA by one-dimensional diffusion and that MutS bends the DNA during its search.[13,18,33] Consequently, it is likely that the initial encounter of MutS with the mismatch occurs via a conformation in which the DNA is bent. Furthermore, a recent SAXS study[16] suggests that DNA distortion is involved in the earliest mispair recognition steps.

The suggestion that MutS−T-bulge complexes undergo a transition from **B** to **U** too quickly for observation upon initial binding is supported by studies of base-flipping enzymes that induce DNA bending prior to DNA unbending and base flipping.[34,35] Studies of the DNA binding properties of uracil DNA glycosylase (UDG) showed that bases lacking base pair hydrogen bonding interactions (such as the T-bulge) are more flexible and have lower bending free energies, and the transition barrier through the bent conformation and into an unbent, base-flipped conformation is reduced by ∼3 kcal/mol relative to that of hydrogen-bonded base pairs.[34] In addition, conformational transitions observed in DNA methyltransferase *Eco*RI showed that the enzyme−DNA complex undergoes a transition from a bent DNA conformation to an unbent, base-flipped DNA conformation within the first 25 ms after binding to the DNA.[35] Consequently, it is likely that MutS binds the T-bulge in the bent state but rapidly undergoes a conformational change to the unbent state, with the transition occurring faster than the time resolution of our experiments. In other words, the lack of observation of bending upon binding can be explained if the rate constant for the transition from **B** to **U** is significantly increased for the T-bulge relative to that of GT (transitions with rates faster than ∼10 s^{-1} would be missed in our experiments). This latter suggestion is consistent with the observed stabilization of **U**, but not **B**, in MutS−T-bulge complexes relative to MutS−GT complexes. An increase in rate of the transition from **B** to **U** is also consistent with the increased population of **I**, because **U** preferentially undergoes the transition to ***I***, and if **I** undergoes the transition to **B**, **B** will rapidly convert to **U**. Transitions from **I** to **U** are rarely observed for MutS−GT complexes because MutS preferentially dissociates from GT when MutS is bound in the **I** conformation.[13] The increased affinity of MutS for a T-bulge relative to that for GT reduces the dissociation rate, which in turn allows transitions from **I** to **U** rather than dissociation of MutS from the DNA, and **I** becomes on path to the formation of **U** for the T-bulge.

Given that the interaction of MutS with a mismatch significantly alters base−base hydrogen bonding,[10] our results suggest that hydrogen bonding between the mismatch bases, in part, inhibits the formation of the signaling state, and the formation of **U** involves disruption of base−base hydrogen bonding. Differences in base stacking interactions between the T-bulge and GT DNA also likely play a role but are difficult to tease apart in this study. These results, taken together with the lack of correlation between the affinity of MutS for a mismatch and its ability to signal repair,[17−21] suggest that differences in hydrogen bonding, as well as base stacking, of mismatches may govern, in part, the efficiency of mismatch repair.

Our results reveal that both the DNA conformations as well as the dynamics of transitions between these conformations play an important role in mismatch recognition and the ability to signal repair. The well-repaired mismatches studied in this work sample a number of different states but follow a preferred pathway that ultimately proceeds to a stable slightly bent/unbent state (**U**). In contrast, complexes whose homologues show poor repair *in vivo* and/or poor signaling *in vitro*, such as MutS with CC or MutS-E41A with GT, do not efficiently proceed through the conformational pathways that lead to the unbent state. Our observations support previous suggestions that an unbent state is a point of entry into the repair pathway.[7,13,18] Thus, a growing set of observations suggests a model in which a progression of conformations from bent to unbent may be an essential step in the signaling that initiates repair. In this model, the more dynamic MutS−DNA complexes could sample the unbent conformation less frequently and yet still be repaired (e.g., MutS-E41A−T-bulge complex) while others that do not sample the unbent

conformation for a sufficient period of time will activate repair less efficiently (e.g., MutS-E41A−GT and MutS−CC complexes), resulting in refractory or decreased mismatch repair.

Finally, our data suggest that the functional pathway we identified is common across three different mismatches despite the wide range of affinities and kinetic rates. Consequently, if this generalization is valid for all mismatches, blocking any conformation that is on the functional pathway can lead to impaired repair. This model, or another such model that addresses molecular details of MMR signaling mechanisms, will provide a framework that may allow the rational design of drugs that could either promote or inhibit the main conformational pathway. The potential of such engineering approaches to redesigning the DNA MMR machinery is foreshadowed by a cysteine mutant of MutSα, which restricted MutSα conformational changes and inhibited the ability of MutSα to signal the downstream events that lead to repair.[36]

■ ASSOCIATED CONTENT

Supporting Information

Supplemental data and figure. This material is available free of charge via the Internet at http://pubs.acs.org.

■ AUTHOR INFORMATION

Corresponding Authors

*Department of Physics, North Carolina State University, Box 8208, Raleigh, NC 27606. Telephone: (919) 513-3696. E-mail: krwening@ncsu.edu.

*Department of Chemistry, The University of North Carolina at Chapel Hill, CB#3290, Chapel Hill, NC 27599. E-mail: derie@unc.edu. Telephone: (919) 962-6370. Fax: (919) 962-2388.

Author Contributions

V.C.D., L.E.S., R.Q., D.A.E., and K.R.W. designed experiments. V.C.D., L.E.S., and R.Q. conducted experiments and performed data analysis. V.C.D., L.E.S., D.A.E., and K.R.W. wrote and edited the manuscript. V.C.D. and L.E.S. contributed equally to this work.

Funding

This work was supported by research scholar grants from the American Cancer Society to K.R.W. (RSG-10-048) and D.A.E. (RSG-03-047-GMC), National Institutes of Health Grants GM079480 to D.A.E. and GM080294 to D.A.E., a fellowship from the Merck Research Laboratories awarded to L.E.S., and National Institute of General Medical Sciences Fellowship F31GM087096 awarded to V.C.D.

Notes

The authors declare no competing financial interests.

■ ABBREVIATIONS

MMR, mismatch repair; HNPCC, hereditary nonpolyposis colorectal cancer; AFM, atomic force microscopy; smFRET, single-molecule Förster resonance energy transfer; MutS, wild-type MutS; BSA, bovine serum albumin; TIRF, total internal reflectance fluorescence; TDP, transition density plot; emCCD, electron-multiplying charge-coupled device; TAMRA, tetramethylrhodamine.

■ REFERENCES

(1) Karran, P., Offman, J., and Bignami, M. (2003) Human mismatch repair, drug-induced DNA damage, and secondary cancer. *Biochimie 85*, 1149−1160.

(2) Bignami, M., Casorelli, I., and Karran, P. (2003) Mismatch repair and response to DNA-damaging antitumour therapies. *Eur. J. Cancer 39*, 2142−2149.

(3) Fedier, A., and Fink, D. (2004) Mutations in DNA mismatch repair genes: Implications for DNA damage signaling and drug sensitivity (review). *Int. J. Oncol. 24*, 1039−1047.

(4) Peltomaki, P. (2003) Role of DNA mismatch repair defects in the pathogenesis of human cancer. *J. Clin. Oncol. 21*, 1174−1179.

(5) Modrich, P. L. (1989) Methyl-directed DNA mismatch correction. *J. Biol. Chem. 264*, 6597−6600.

(6) Loeb, L. A., Loeb, K. R., and Anderson, J. P. (2003) Multiple mutations and cancer. *Proc. Natl. Acad. Sci. U.S.A. 100*, 776−781.

(7) Kunkel, T. A., and Erie, D. A. (2005) DNA mismatch repair. *Annu. Rev. Biochem. 74*, 681−710.

(8) Iyer, R. R., Pluciennik, A., Burdett, V., and Modrich, P. L. (2006) DNA mismatch repair: Functions and mechanisms. *Chem. Rev. 106*, 302−323.

(9) Lamers, M. H., Perrakis, A., Enzlin, J. H., Winterwerp, H. H., de Wind, N., and Sixma, T. K. (2000) The crystal structure of DNA mismatch repair protein MutS binding to a G × T mismatch. *Nature 407*, 711−717.

(10) Natrajan, G., Lamers, M. H., Enzlin, J. H., Winterwerp, H. H., Perrakis, A., and Sixma, T. K. (2003) Structures of *Escherichia coli* DNA mismatch repair enzyme MutS in complex with different mismatches: A common recognition mode for diverse substrates. *Nucleic Acids Res. 31*, 4814−4821.

(11) Obmolova, G., Ban, C., Hsieh, P., and Yang, W. (2000) Crystal structures of mismatch repair protein MutS and its complex with a substrate DNA. *Nature 407*, 703−710.

(12) Warren, J. J., Pohlhaus, T. J., Changela, A., Iyer, R. R., Modrich, P. L., and Beese, L. S. (2007) Structure of the Human MutSα DNA Lesion Recognition Complex. *Mol. Cell 26*, 579−592.

(13) Wang, H., Yang, Y., Schofield, M. J., Du, C., Fridman, Y., Lee, S. D., Larson, E. D., Drummond, J. T., Alani, E., Hsieh, P., and Erie, D. A. (2003) DNA bending and unbending by MutS govern mismatch recognition and specificity. *Proc. Natl. Acad. Sci. U.S.A. 100*, 14822−14827.

(14) Sass, L. E., Lanyi, C., Weninger, K. R., and Erie, D. A. (2010) Single-molecule FRET TACKLE reveals highly dynamic mismatched DNA-MutS complexes. *Biochemistry 49*, 3174−3190.

(15) Cristovao, M., Sisamakis, E., Hingorani, M. M., Marx, A. D., Jung, C. P., Rothwell, P. J., Seidel, C. A., and Friedhoff, P. (2012) Single-molecule multiparameter fluorescence spectroscopy reveals directional MutS binding to mismatched bases in DNA. *Nucleic Acids Res. 40*, 5448−5464.

(16) Hura, G. L., Tsai, C. L., Claridge, S. A., Mendillo, M. L., Smith, J. M., Williams, G. J., Mastroianni, A. J., Alivisatos, A. P., Putnam, C. D., Kolodner, R. D., and Tainer, J. A. (2013) DNA conformations in mismatch repair probed in solution by X-ray scattering from gold nanocrystals. *Proc. Natl. Acad. Sci. U.S.A. 110*, 17308−17313.

(17) Su, S. S., Lahue, R. S., Au, K. G., and Modrich, P. (1988) Mispair specificity of methyl-directed DNA mismatch correction in vitro. *J. Biol. Chem. 263*, 6829−6835.

(18) Tessmer, I., Yang, Y., Zhai, J., Du, C., Hsieh, P., Hingorani, M. M., and Erie, D. A. (2008) Mechanism of MutS searching for DNA mismatches and signaling repair. *J. Biol. Chem. 283*, 36646−36654.

(19) Groothuizen, F. S., Fish, A., Petoukhov, M. V., Reumer, A., Manelyte, L., Winterwerp, H. H., Marinus, M. G., Lebbink, J. H., Svergun, D. I., Friedhoff, P., and Sixma, T. K. (2013) Using stable MutS dimers and tetramers to quantitatively analyze DNA mismatch recognition and sliding clamp formation. *Nucleic Acids Res. 41*, 8166−8181.

(20) Holmes, S. F., Scarpinato, K. D., McCulloch, S. D., Schaaper, R. M., and Kunkel, T. A. (2007) Specialized mismatch repair function of Glu339 in the Phe-X-Glu motif of yeast Msh6. *DNA Repair 6*, 293−303.

(21) Lebbink, J. H., Georgijevic, D., Natrajan, G., Fish, A., Winterwerp, H. H., Sixma, T. K., and de Wind, N. (2006) Dual role

of MutS glutamate 38 in DNA mismatch discrimination and in the authorization of repair. *EMBO J. 25*, 409−419.
(22) Jiricny, J. (2000) Mismatch repair: The praying hands of fidelity. *Curr. Biol. 10*, R788−R790.
(23) Biswas, I., and Hsieh, P. (1996) Identification and characterization of a thermostable MutS homolog from *Thermus aquaticus*. *J. Biol. Chem. 271*, 5040−5048.
(24) Li, Y., Augustine, G. J., and Weninger, K. (2007) Kinetics of complexin binding to the SNARE complex: Correcting single molecule FRET measurements for hidden events. *Biophys. J. 93*, 2178−2187.
(25) Canny, J. (1986) A computational approach to edge detection. *IEEE Transactions on Pattern Analysis and Machine Intelligence 8*, 679−698.
(26) McKinney, S. A., Joo, C., and Ha, T. (2006) Analysis of single-molecule FRET trajectories using hidden Markov modeling. *Biophys. J. 91*, 1941−1951.
(27) Schofield, M. J., Brownewell, F. E., Nayak, S., Du, C., Kool, E. T., and Hsieh, P. (2001) The Phe-X-Glu DNA binding motif of MutS. The role of hydrogen bonding in mismatch recognition. *J. Biol. Chem. 276*, 45505−45508.
(28) Cho, M., Chung, S., Heo, S. D., Ku, J., and Ban, C. (2007) A simple fluorescent method for detecting mismatched DNAs using a MutS-fluorophore conjugate. *Biosens. Bioelectron. 22*, 1376−1381.
(29) Boulard, Y., Cognet, J. A., and Fazakerley, G. V. (1997) Solution structure as a function of pH of two central mismatches, C·T and C·C, in the 29 to 39 K-ras gene sequence, by nuclear magnetic resonance and molecular dynamics. *J. Mol. Biol. 268*, 331−347.
(30) Yang, Y., Sass, L. E., Du, C., Hsieh, P., and Erie, D. A. (2005) Determination of protein-DNA binding constants and specificities from statistical analyses of single molecules: MutS-DNA interactions. *Nucleic Acids Res. 33*, 4322−4334.
(31) Jiricny, J., Su, S. S., Wood, S. G., and Modrich, P. (1988) Mismatch-containing oligonucleotide duplexes bound by the *E. coli* mutS-encoded protein. *Nucleic Acids Res. 16*, 7843−7853.
(32) Brown, J., Brown, T., and Fox, K. R. (2001) Affinity of mismatch-binding protein MutS for heteroduplexes containing different mismatches. *Biochem. J. 354*, 627−633.
(33) Gorman, J., Chowdhury, A., Surtees, J. A., Shimada, J., Reichman, D. R., Alani, E., and Greene, E. C. (2007) Dynamic basis for one-dimensional DNA scanning by the mismatch repair complex Msh2-Msh6. *Mol. Cell 28*, 359−370.
(34) Krosky, D. J., Song, F., and Stivers, J. T. (2005) The origins of high-affinity enzyme binding to an extrahelical DNA base. *Biochemistry 44*, 5949−5959.
(35) Youngblood, B., and Reich, N. O. (2006) Conformational transitions as determinants of specificity for the DNA methyltransferase EcoRI. *J. Biol. Chem. 281*, 26821−26831.
(36) Hargreaves, V. V., Putnam, C. D., and Kolodner, R. D. (2012) Engineered disulfide-forming amino acid substitutions interfere with a conformational change in the mismatch recognition complex Msh2-Msh6 required for mismatch repair. *J. Biol. Chem. 287*, 41232−41244.